degradation is attractive from the implementation point of view since the computational complexity of the brute-force search user selection for this scenario is 2.36 times higher than the sum rate-based user selection. Similar conclusions can be extended to the second scenario. It is also shown that the performance of the THP-ZF scheme with LC-PA is only 0.2 bit/s/Hz lower than the performance of Opt-PA for both scenarios. This means that the power allocation at the BS plays the dominant role in the SINR expression in (2), whereas the power allocation at the RS does not. In addition, the computational complexity of LC-PA in (7) is significantly lower than Opt-PA in (5). Note that the sum rate of 6.92 and 7.33 bit/s/Hz for two-user system with the proposed THP-ZF scheme, LC-PA, and brute-force search user selection under the first and second scenarios at $\sigma^2 = -140$ dB are equivalent to the SINRs of 20.8 and 22 dB for each user, respectively.

VII. Conclusion

In this paper, we have proposed a practical precoding, beamforming, and relaying scheme with power allocation for MU-MIMO relay networks. An iterative THP-ZF scheme has been developed to cancel multiuser interference. An LC-PA technique that maximizes the minimum SINR of all users to achieve data rate fairness among different users has been proposed. In addition, the problem of choosing a subset of users that has the best overall sum rate performance has been investigated. We have shown by simulation results that the iterative THP-ZF outperforms the scheme in [3], where a combination of zero-forcing beamforming and dirty paper coding is used to cancel the interference. It is also shown that the performance of the iterative THP-ZF with the LC-PA is very close to the performance of the iterative THP-ZF with the optimal power allocation but with lower complexity. In addition, the simulation results indicate that the performance of the proposed low-complexity user selection algorithm is very close to the performance of a user selection based on exhaustive search of all the possible user sets.

References

[1] C. Windpassinger, R. F. H. Fischer, T. Vencel, and J. B. Huber, "Precoding in multiantenna and multiuser communications," *IEEE Trans. Wireless Commun.*, vol. 3, no. 4, pp. 1305–1316, Jul. 2004.

[2] T. Yoo and A. Goldsmith, "Optimality of zero-forcing beamforming with multiuser diversity," in *Proc. IEEE Int. Conf. Commun.*, May 2005, pp. 542–546.

[3] C. Chae, T. Tang, R. W. Heath, and S. Cho, "MIMO relaying with linear processing for multiuser transmission in fixed relay networks," *IEEE Trans. Signal Process.*, vol. 56, no. 2, pp. 727–738, Feb. 2008.

[4] R. Zhang, C. Chai, and Y. Liang, "Joint beamforming and power control for multiantenna relay broadcast channel with QoS constraints," *IEEE Trans. Signal Process.*, vol. 57, no. 2, pp. 726–737, Feb. 2009.

[5] N. D. Dao and Y. Sun, "User-selection algorithms for multiuser precoding," *IEEE Trans. Veh. Technol.*, vol. 59, no. 7, pp. 3617–3622, Sep. 2010.

[6] Z. Shen, R. Chen, J. G. Andrews, R. W. Heath, and B. L. Evans, "Low complexity user selection algorithms for multiuser MIMO systems with block diagonalization," *IEEE Trans. Signal Process.*, vol. 54, no. 9, pp. 3658–3663, Sep. 2006.

[7] A. Wolfgang, N. Seifi, and T. Ottosson, "Resource allocation and linear precoding for relay assisted multiuser MIMO systems," in *Proc. Int. ITG Workshop Smart Antennas*, Feb. 2008, pp. 162–168.

[8] O. Oyman and A. J. Paulraj, "Design and analysis of linear distributed MIMO relaying algorithms," *Proc. Inst. Elect. Eng.—Commmun.*, vol. 153, no. 4, pp. 565–572, Aug. 2006.

[9] M. Tomlinson, "New automatic equalizer employing modulo arithmetic," *Electron. Lett.*, vol. 7, no. 5, pp. 138–139, Mar. 1971.

[10] M. Miyakawa and H. Harashima, "A method of code conversion for a digital communication channel with intersymbol interference," *Trans. Inst. Electron. Commun. Eng. Jpn.*, vol. 52-A, pp. 272–273, Nov. 1971.

[11] W. Hardjawana, B. Vucetic, and Y. Li, "Cooperative precoding and beamforming for co-existing multi-user MIMO systems," in *Proc. IEEE ICC*, 2009, pp. 1–5.

[12] A. Wiesel, Y. C. Eldar, and S. Shamai, "Linear precoding via conic optimization for fixed MIMO receivers," *IEEE Trans. Signal Process.*, vol. 54, no. 1, pp. 161–176, Jan. 2006.

[13] S. Boyd and L. Vandenberghe, *Convex Optimization*. Cambridge, U.K.: Cambridge Univ. Press, 2004.

[14] G. H. Golub and C. F. V. Loan, *Matrix Computations*. Baltimore, MD: The Johns Hopkins Univ. Press, 1996.

[15] J. C. Bezdek and R. J. Hathaway, "Some notes on alternating optimization," *Adv. Soft Comput.—AFSS*, ser. LNCS, vol. 2275, no. 4, pp. 187–195, 2002.

[16] W. Yang and G. Xu, "Optimal downlink power assignment for smart antenna systems," in *Proc. IEEE ICASSP*, 1998, pp. 3337–3340.

[17] "WINNER II channel models," Information Society Technologies, Tech. Rep. IST-4-027756, WINNER II D1.1.2 V1.2, Sep. 2007.

A Cumulant-Based Investigation of the Impact of Secondary Users' Field Size on Spectrum-Sharing Opportunities

Muhammad Aljuaid and Halim Yanikomeroglu

***Abstract*—Previous works studied the effect of different system parameters on spectrum-sharing opportunities where secondary users access the spectrum of primary users (PUs). However, a parameter that has received little attention is the spatial size of the field of secondary users. Usually, the field size is assumed to be infinite. Using results developed for infinite fields might be too pessimistic, leading to missing spectrum-sharing opportunities. This paper studies the effect of field size on spectrum-sharing opportunities. We verify that asymptotic results obtained for infinite fields are applicable for finite but relatively large fields (when the radial depth of the field is much greater than the minimum distance to the PU) as well. We also demonstrate that, in some cases, however, asymptotic results are too pessimistic, hiding some spectrum-sharing opportunities. Moreover, this paper shows that, in certain situations, a small reduction in the field size may create spectrum-sharing opportunities, while in certain other situations, a huge increase in the field size may not eliminate spectrum-sharing opportunities. Our study is based on a cumulant-based characterization of the aggregate interference power generated by secondary users. A number of recent papers in literature have dealt with cumulants of the aggregate interference, but only under specific scenarios. We introduce a more comprehensive method to determine the cumulants under various system and channel conditions. These cumulants are utilized to understand the dynamics of the aggregate interference power, approximate its distribution, and, hence, investigate the spectrum-sharing opportunities.**

***Index Terms*—Aggregate interference, cumulants, fading, interference probability, Poisson point process, spectrum sharing.**

Manuscript received April 12, 2010; revised November 29, 2010 and April 2, 2011; accepted May 6, 2011. Date of publication June 27, 2011; date of current version September 19, 2011. This work was presented in part at the 2010 IEEE Wireless Communications and Networking Conference (WCNC) [1] and at the 2010-Spring IEEE Vehicular Technology Conference (VTC) [2]. This work was supported in part by Saudi Aramco, Dhahran, Saudi Arabia. The review of this paper was coordinated by Dr. E. K. S. Au.

M. Aljuaid was with Carleton University, Ottawa, ON K1S 5B6, Canada. He is now with Saudi Aramco, Dhahran 31311, Saudi Arabia (e-mail: mjuaid@gmail.com).

H. Yanikomeroglu is with the Department of Systems and Computer Engineering, Carleton University, Ottawa, ON K1S 5B6, Canada (e-mail: halim@sce.carleton.ca).

Color versions of one or more of the figures in this paper are available online at http://ieeexplore.ieee.org.

Digital Object Identifier 10.1109/TVT.2011.2160665

I. Introduction

A Federal Communications Commission proposal on spectrum sharing [3] has stimulated significant interest in academia and industry due to its potential in reducing the effect of radio spectrum scarcity. In the spectrum-sharing proposal, a secondary user (likely an unlicensed user) could share the spectrum with a primary user (PU, licensed user), provided that the operation of the secondary user does not introduce "harmful interference" toward the PU [3].

Some metrics have been proposed in the literature to identify whether the interference generated by secondary users reaches to a level of being "harmful" to the PUs [4]–[6]. Works such as [4]–[6] study the effect of various system parameters on the harmful interference metric. However, a system parameter that has not received much attention is the spatial size of the field of secondary users. In most studies, the spatial size of the field (or simply the "field size") is assumed to be infinite. However, since the spectrum sharing is opportunistic, using results developed for an infinite field might be too pessimistic, leading to missing spectrum-sharing opportunities. This concern about the applicability of the results of infinite fields could be properly addressed by studying the behavior of the harmful interference metric and, hence, the spectrum-sharing opportunities, with respect to the changes in the field size. To facilitate this study, the aggregate interference power should be characterized first.

Many papers investigate the characterization of the aggregate interference power by modeling the wireless network as a Poisson field of independent interferers. Further history and references are provided in [7] and [8]. Closed-form expressions for the characteristic function of the aggregate interference power are achievable. However, the inversion of this characteristic function into a closed-form probability density function (pdf) or cumulative distribution function (cdf) is not achievable, except for a few cases. A viable option to overcome this inversion problem is to obtain moments (or cumulants) of the aggregate interference and then to apply moment-based (or cumulant-based) approximations or bounds [4], [6], [9]–[11].

While the moments and cumulants are closely related, cumulants have some properties that make them more attractive for characterizing the aggregate interference of a Poisson field of interferers. To the best of our knowledge, few papers in literature have dealt with cumulants of the aggregate interference power. These papers focus on specific scenarios. For example, Menon *et al.* [4], [11] dealt with cumulants for nonfading scenarios, Chan and Hanly [10] provided an integral form to compute the cumulants for out-of-cell interference in a code-division multiple-access networks, and Ghasemi and Sousa [6] considered an infinite field with an exclusion region. Extending these results and generalizing them for a wide range of scenarios are among the contributions of this paper.

We characterize the distribution of the aggregate interference using cumulants.[1] We provide a very simple yet powerful method to determine the cumulants. The method is flexible enough to be applicable to a wide range of scenarios including, but not limited to, the following: finite fields, infinite fields, different small-scale and large-scale fading distributions (e.g., Rayleigh, Rician, lognormal, and generalized-K), and variations in power levels. As another contribution, we investigate the behavior of cumulants and, hence, the aggregate interference power, with respect to changes in the network size and for various fading distributions. Furthermore, we study how the interference probability and, correspondingly, the spectrum-sharing opportunities would change with changes in the field size.

[1]The cumulant-based approach turns out to be very helpful in investigating the characteristics of the aggregate interference. For example, Aljuaid and Yanikomeroglu [12] investigated the Gaussianity of the aggregate interference power based on results obtained from cumulant-based characterization.

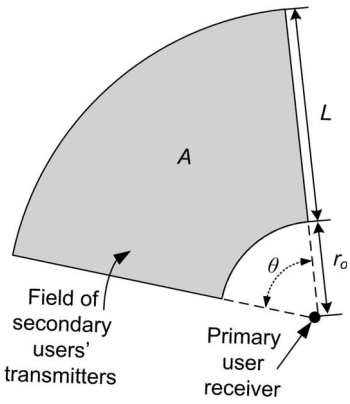

Fig. 1. Field layout.

The rest of this paper is organized as follows: Section II describes the system model used in this paper. Section III presents a simple method for calculating the cumulants of the aggregate interference power. The effects of the network size and fading distributions on cumulants are investigated in Sections IV and V, respectively. Section VI discusses the cumulant-based approximations of the distribution of the aggregate interference power. The effect of the field size on the spectrum-sharing opportunities is discussed in Section VII. In Section VIII, we extend our discussion on spectrum sharing to a field with irregular shape or a field of heterogeneous secondary networks. Finally, Section IX summarizes the main results in this paper.

II. System Model

The analysis in this paper is based on modeling a secondary network as a 2-D field of interferers deployed over a region of area A with an annular sector shape. (Ring or disk shapes are special cases.) The set of active secondary user transmitters (SU-TXs) is assumed to follow a Poisson point process with a homogeneous density λ. The field of SU-TXs is assumed to have an inner radius of r_o. We call the disk $b(O, r_o)$ of radius r_o and centered at the origin "exclusion region." The field has a radial depth of L, making the outer radius of the field $r_o + L$. The field spans over an angle of θ, as seen by the victim receiver at the origin, as shown in Fig. 1.

The individual interference power received by a PU receiver (PU-RX) at the origin due to the transmission of node i is denoted by I_i. Under the assumption of incoherent addition of interfering signals, the aggregate interference power received by the PU-RX can be expressed as

$$I_A = \sum_{i \in \Lambda} I_i = \sum_{i \in \Lambda} X_i g(r_i) \tag{1}$$

where Λ is a set of active SU-TXs, and X_i is a positive random variable that can be modeled as the multiplication of deterministic quantities and various random variables reflecting the transmit power, antenna gain, channel attenuation (including multipath and shadow fading) and other factors. In analyzing the aggregate interference of a Poisson field, it is common to assume that X_i's are independent and identically distributed (i.i.d.) random variables [4], [6], [7]. In this paper, we follow the same assumption. Function $g(r_i)$ represents a path-loss model (or, more precisely, the distance-dependent attenuation).

Inaltekin *et al.* [13] indicated that more realistic performance figures are obtained by using nonsingular (bounded) path-loss models. Therefore, our results in this paper is based on the following nonsingular model:

$$g(r_i) = \begin{cases} kr_i^{-n}, & r_i \geq r_c \\ kr_c^{-n}, & r_i < r_c \end{cases} \tag{2}$$

where k is a constant, r_i is the distance between SU-TX i and the PU-RX, n is the path-loss exponent, and $r_c > 0$ is the radius at which the slope of the model starts changing. We consider $n > 2$ as commonly assumed in similar works. Without loss of generality, we take $k = 1$, assuming that its effect is absorbed by X_i.

The harmful interference metric that is used in this paper is the interference probability, i.e.,

$$P(I_A \geq I_{\text{th}}) \leq \beta \tag{3}$$

which means that the probability of the aggregate interference being greater than a certain interference threshold I_{th} should not exceed β, where $\beta \ll 1$ [6]. If (3) is not violated, then the aggregate interference is considered to be nonharmful. We choose this metric because it has a fundamental and versatile form, which is mainly based on the complimentary cdf (CCDF). Thus, results of this paper should be useful, even if different metrics are used, provided that these metrics depend on the distribution function of I_A.

We are interested in studying how the interference probability and, hence, the spectrum sharing behave with respect to changes in the field size, mainly L. To achieve this, the distribution of I_A or at least some of its characteristics are required. In this paper, we characterize the aggregate interference power using its cumulants.

III. Cumulants of I_A

One of the contributions of this paper is stated in the following proposition: To value this proposition, it is helpful to imagine that the field of interferers would virtually collapse to a subfield with an effective area A_{eff}, an inner radius r_o, and an outer radius r_{eff}. The average number of interfering nodes within this subfield is N_{eff}.

Proposition 1: The mth cumulant of the distribution of the aggregate interference power received by a victim receiver at the origin from an annulus-shaped Poisson field of i.i.d. interferers is

$$\kappa_m(I_A) = N_{\text{eff}}(m)\tilde{\mu}_m(I_{r_o}) \tag{4}$$

where $N_{\text{eff}}(m)$ is the average number of interfering nodes within a radius of $r_{\text{eff}}(m)$ from the victim receiver, and $\tilde{\mu}_m(I_{r_o})$ is the mth raw moment of the distribution of the interference power received by the victim receiver from an interfering node at distance r_o. We then have

$$N_{\text{eff}}(m) = \lambda A_{\text{eff}}(m) \tag{5}$$

$$A_{\text{eff}}(m) = \frac{1}{2}\theta\left[r_{\text{eff}}^2(m) - r_o^2\right] \tag{6}$$

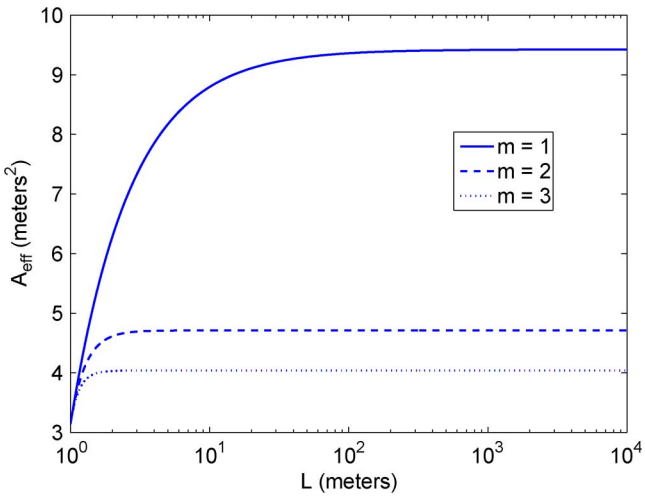

Fig. 2. Effect of L on A_{eff} and, hence, on κ_m for the case of no exclusion region around the PU-RX ($r_c = 1$ m, $\theta = 2\pi$, and $n = 3$).

$$r_{\text{eff}}(m) = \hat{r}\sqrt{1 + \frac{2}{mn-2}\left(1 - \left[\frac{\hat{r}}{r_o + L}\right]^{mn-2}\right)}$$
$$\hat{r} = \max\left(\min(r_c, r_o + L), r_o\right). \tag{7}$$

Note that

$$\tilde{\mu}_m(I_{r_o}) = \tilde{\mu}_m(X)\left[g(r_o)\right]^m \tag{8}$$

where $\tilde{\mu}_m(X)$ is the mth raw moment of X_i.

Proof: See [2]. ■

Equation (4) is simple yet flexible in the sense that it can be applied to a wide range of scenarios such as finite fields, infinite fields (see Section IV), and different fading distributions (see Section V). Moreover, (4) is applicable for many field's topologies, including when the PU-RX is at the middle of a secondary network or away from it. Equations (5)–(7) can be combined to express κ_m in an expanded form as in (9), shown at the bottom of the page.

IV. Effect of the Spatial Size of the Field and Secondary User Transmitter Density on Cumulants

The spatial size of the field is controlled by L, r_o, and θ. The changes in L affect r_{eff} and, hence, A_{eff} and κ_m. However, this effect is limited. As L increases, r_{eff} increases, but it converges to a finite value, regardless of further increase in L. As m or n increases, this convergence occurs faster. The effect of changes in L is significant only for lower order cumulants and for L closer to or less than $\max(r_c, r_o)$. As L approaches the value of $\max(r_c, r_o)$, its effect becomes weaker, and it will be negligible when $(\max(r_c, r_o)/(r_o + L))^{mn-2} \ll 1$ (see Figs. 2 and 3). Interestingly, the value of r_{eff} converges to $\max(r_c, r_o)\sqrt{1 + (2/(mn-2))}$ as $L \to \infty$. From this, we may conclude that κ_m is mainly controlled by the region that is close to the victim receiver. The dominant region for κ_1 (the average)

$$\kappa_m(I_A) = \begin{cases} \frac{\lambda\theta\tilde{\mu}_m(X)r_o^{2-mn}}{nm-2}\left[1 - \left(\frac{r_o}{r_o+L}\right)^{mn-2}\right], & \text{for } 0 < r_c \leq r_o \leq r_o + L \\ \frac{1}{2}\lambda\theta\tilde{\mu}_m(X)r_c^{-mn}\left[r_c^2 - r_o^2\right] + \frac{\lambda\theta\tilde{\mu}_m(X)r_c^{2-mn}}{nm-2}\left[1 - \left(\frac{r_c}{r_o+L}\right)^{mn-2}\right], & \text{for } 0 \leq r_o < r_c \leq r_o + L \\ \frac{1}{2}\lambda\theta\tilde{\mu}_m(X)r_c^{-mn}\left[(r_o + L)^2 - r_o^2\right], & \text{for } 0 \leq r_o \leq r_o + L < r_c \end{cases} \tag{9}$$

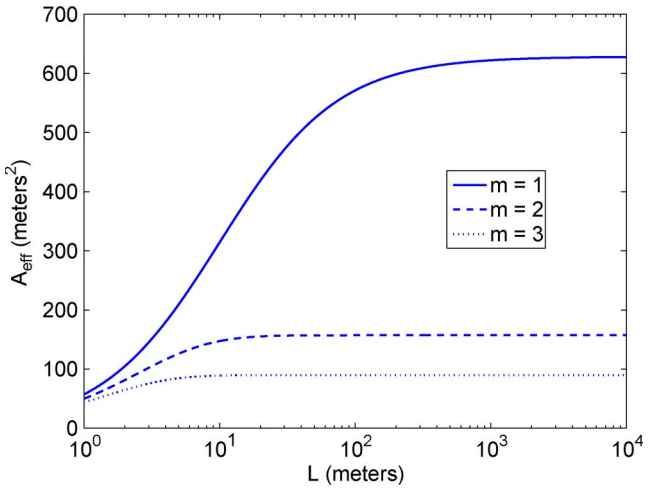

Fig. 3. Effect of L on A_{eff} and, hence, on κ_m for the case of an exclusion region of $r_o = 10$ m ($r_c = 1$ m, $\theta = 2\pi$, and $n = 3$).

is wider than that for κ_2 (the variance). It shrinks as m increases. On the other hand, this dominant region expands as r_o (the exclusion region) increases. The exclusion region has an effect on A_{eff} of an order of r_o^2 (provided that $r_o > r_c$). Moreover, r_o affects the value of $\tilde{\mu}_m(I_{r_o})$ by an order of r_o^{-mn}. Therefore, the net effect of r_o on κ_m is on the order of r_o^{2-mn}, which suggests that increasing the value of r_o is an effective way to lower the aggregate interference. However, increasing r_o may contradict the performance objectives of the wireless network [11], [14]. Therefore, an optimal tradeoff is to be found.

Regarding the effect of the active node density (λ), it has a linear effect on all cumulants. Therefore, it is one of the important parameters that could be used to control the level of interference at the PU-RX. Similarly, θ has a linear effect on the cumulants. However, it is limited to the range $[0, 2\pi]$. It may reflect the effectiveness of using a directional antenna at the PU-RX.

V. Effect of the Distribution of X on Cumulants

The random variable X encompasses many system and channel parameters. It might be modeled as the multiplication of some deterministic and random variables, reflecting the effect of different parameters, such as fluctuations in power level and antenna gains, multipath fading, and shadow fading[2]

$$X_i = \prod_l X_{i,l} \tag{10}$$

where $X_{i,l}$ is a deterministic or a random variable. (A similar representation is used in [7].)

From (4) and $\tilde{\mu}_m(I_{r_o}) = \tilde{\mu}_m(X)[g(r_o)]^m$, it is clear that the distribution of X_i has a major influence on κ_m and, hence, the distribution of the aggregate interference power. A similar observation on the influence of the fading distribution, equivalently of the distribution of X_i, on the aggregate interference appears in [16].

Appendix A shows some examples of κ_m under different distributions of X_i. These examples consider fading distributions only; however, X_i in our model is more general than just fading.

[2]Equation (10) is general enough to account for the adjacent-channel interference (see [15]).

VI. Cumulant-Based Approximations of the Distribution of I_A

The distribution of I_A can be approximated using a finite set of its cumulants. Some examples are given here.

Edgeworth series expansion: The Edgeworth series expansion is used in [4], [6], and [10] to approximate the pdf of the aggregate interference. An approximation of the pdf of I_A based on this approach and using the first few cumulants can be written as

$$f_{\tilde{I}_A}(y) \simeq f_{\text{nd}}(y)\left[1 + \frac{\tilde{\kappa}_3(I_A)}{6}H_3(y) + \frac{\tilde{\kappa}_4(I_A)}{24}H_4(y) + \frac{\tilde{\kappa}_3^2(I_A)}{72}H_6(y)\right] \tag{11}$$

where $\tilde{I}_A = (I_A - \kappa_1(I_A))/\kappa_2^{1/2}(I_A)$ is the standardized I_A, $f_{\text{nd}}(y)$ is the standard normal pdf, and $\tilde{\kappa}_m$ are the mth standardized cumulants, which are equal to $(\kappa_m/\kappa_2^{m/2})$ for $m \geq 2$ and 0 for $m = 1$. $H_m(y)$ are the Hermite polynomials, which are defined by $H_m(y) = (-1)^m f_{\text{nd}}(y)^{-1}(d^m/dy^m)f_{\text{nd}}(y)$. The (outage) interference probability can be calculated as

$$P(I_A \geq I_{\text{th}}) = P(\tilde{I}_A \geq \tilde{I}_{\text{th}}) = \int_{\tilde{I}_{\text{th}}}^{\infty} f_{\tilde{I}_A}(y)\,dy \tag{12}$$

where $\tilde{I}_{\text{th}} = (I_{\text{th}} - \kappa_1(I_A))/\sqrt{\kappa_2(I_A)}$. While the Edgeworth series expansion is an asymptotic expansion for the pdf, the finite Edgeworth series should be applied with some caution: it is applicable for moderately skewed distributions only. Conditions under which the Edgeworth finite approximation can be used are discussed in [17].

Shifted lognormal: If the distribution of the aggregate interference has a positive skewness, I_A can be approximated by a lognormal random variable. An enhanced version of the lognormal approximation called shifted lognormal approximation is a three-parameter approximation [6]. These parameters are obtained from the first three cumulants. To implement this approximation for the distribution of I_A, let Z denotes the shifted lognormal random variable whose pdf can be written as

$$f_Z(z) = \frac{1}{s(z-b)\sqrt{2\pi}}e^{-(\ln(z-b)-u)^2/2s^2}, \qquad z > b \tag{13}$$

where $s^2 = \ln\tau$, $u = (1/2)\ln(\kappa_2(I_A)/\tau(\tau-1))$, $b = \kappa_1(I_A) - \sqrt{\kappa_2(I_A)/(\tau-1)}$, $\tau = [\upsilon + \sqrt{\upsilon^2 - 1}]^{1/3} + [\upsilon - \sqrt{\upsilon^2 - 1}]^{1/3} - 1$, $\upsilon = 1 + (1/2)\rho^2$, and $\rho = \kappa_3(I_A)/[\kappa_2(I_A)]^{3/2}$. Therefore, the (outage) interference probability can be approximated as

$$P(I_A \geq I_{\text{th}}) \simeq Q\left(\frac{\ln(I_{\text{th}} - b) - u}{s}\right). \tag{14}$$

Figs. 4 and 5 compare the performance of different approximating distributions with respect to Monte Carlo simulation for fading and nonfading scenarios, respectively. Edgeworth series expansion, shifted lognormal, and Gamma approximations work well for the nonfading case. However, if we go deep in the upper tail, the Edgeworth series approximation deviates. The performance of the shifted lognormal and Gamma approximations continue to provide good approximations. Introducing shadow fading increases the skewness of the distribution of

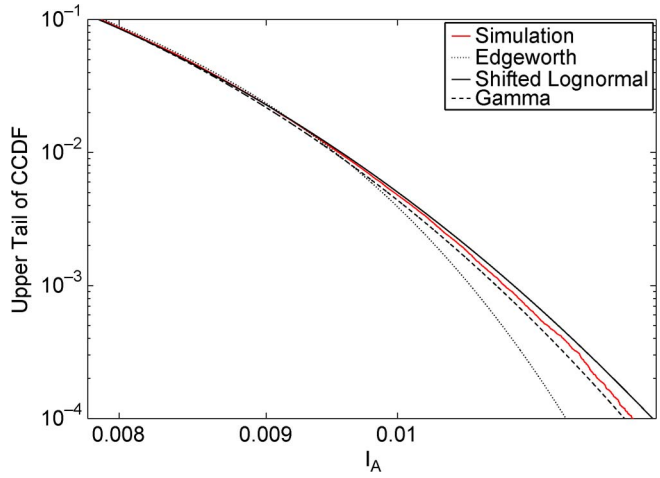

Fig. 4. Upper tail of the CCDF of I_A (with $r_o = 10$ m, $L = 1000$ m, $n = 3$, $\lambda = 0.01$ node/m^2, $\theta = 2\pi$, no multipath fading, and no shadow fading).

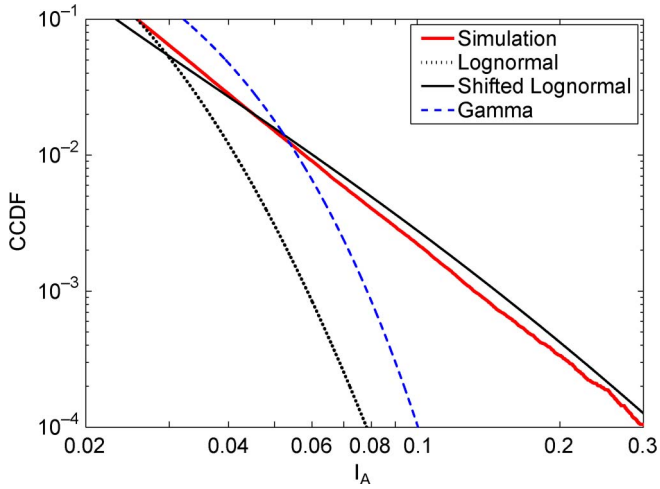

Fig. 5. Upper tail of the CCDF of I_A ($r_o = 10$ m, $L = 1000$ m, $n = 3$, $\lambda = 0.01$ node/m^2, $\theta = 2\pi$, Rayleigh fading, and 6-dB shadow fading). The curve of the Edgeworth approximation is excluded because it fails to generate a valid CCDF curve for heavily skewed distributions. We show a lognormal approximation instead.

I_A and makes it a heavy-tailed distribution. As a result, the Edgeworth series expansion fails to approximate the distribution; it generates a pdf with negative values. Therefore, we exclude it from Fig. 5. The Gamma distribution also does not provide a good approximation when the distribution of I_A has a heavy tail. The shifted lognormal distribution, on the other hand, provides an acceptable approximation of the upper tail of the distribution of I_A, as shown in Fig. 5. In this paper, we focus more on the interference probability as the metric for the spectrum sharing; therefore, the upper tail of the CCDF is more relevant than the body.

VII. Effect of Field Size on Spectrum-Sharing Opportunities

Since spectrum-sharing opportunities are identified by the interference probability, which is in the form of the CCDF of I_A, it is worthwhile discussing the effect of the field size, mainly L, on the distribution of I_A.

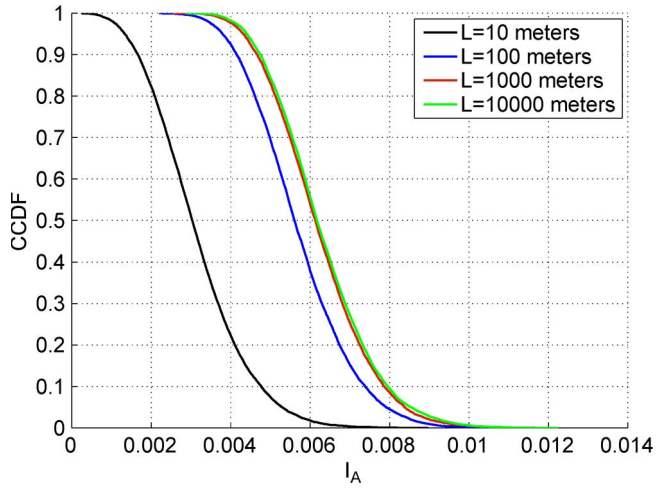

Fig. 6. Monte Carlo-simulation-based CCDF of I_A for different values of L ($r_o = 10$ m, $n = 3$, $r_c = 1$ m, $\theta = 2\pi$, and $\lambda = 0.01$ node/m^2).

A. Effect of Field Size on the Distribution of I_A

It has been shown in previous sections that the cumulants of the distribution of I_A converge to constant values with the increase in L. Moreover, it has been demonstrated that a subset of these cumulants can be used to approximate the distribution. Therefore, it can be expected that the distribution of I_A converges to a limiting distribution with the increase in L. This convergence behavior can be deduced from (11) for the Edgeworth approximation of the pdf of I_A. The Edgeworth approximation considered here depends on the first four cumulants. Since these cumulants exhibit convergence behavior, as shown in Fig. 2, the pdf expression will change with the increase in L but to some extent. Further increase in L will have negligible effect on the distribution of I_A. Similar conclusion can be obtained by investigating the shifted-lognormal approximation in (13). Fig. 6 shows simulation results supporting this conclusion. From this figure, the CCDF curve shifts to the right with the increase in L. However, for a sufficiently large value of L, further increase in L has negligible effect.

B. Effect of Field Size on the Interference Probability

Our investigation on the effect of field size on the interference probability will be based on interference probability expression obtained by approximating the distribution of I_A by a shifted lognormal distribution. This distribution is selected because, as indicated before, it provides a good approximation (particularly for the upper tail, which is of our interest for the interference probability) over a wide range of different system and channel parameters. Equation (14) can be rewritten as

$$P(I_A \geq I_{\text{th}}) \simeq Q\left(\frac{1}{\sqrt{\ln(\tau)}} \ln\left(\sqrt{\tau}\left[\sqrt{\tau-1}\left(\frac{I_{\text{th}}-\kappa_1}{\sqrt{\kappa_2}}\right)+1\right]\right)\right). \tag{15}$$

Based on the expressions of shifted lognormal parameters given in Section VI, it can be shown that τ depends only on the skewness of I_A, i.e., $\rho = \kappa_3(I_A)/[\kappa_2(I_A)]^{3/2}$. Appendix B discusses the skewness of I_A in more detail, including the effect of L. The interference probability in (15) is shown in Fig. 7 for different values of I_{th}. This figure reflects the effect of the increase in L. As L increases, the interference probability converges to a constant value, which can be explained as follows: The expression of the interference probability

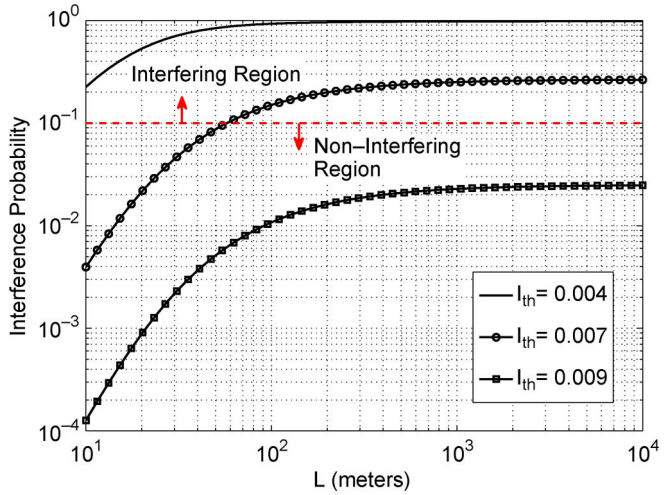

Fig. 7. Field size and spectrum-sharing opportunities ($r_o = 10$ m, $n = 3$, $r_c = 1$ m, $\theta = 2\pi$, $\lambda = 0.01$ node/m^2, no multipath fading, and no shadow fading). The dashed line corresponds to $P_{\rm int} = \beta = 0.1$, which divides the figure into two regions: a noninterfering region (the lower part of the figure) and an interfering region (the upper part of the figure).

in (15) depends on the first three cumulants. The second and third cumulants converge faster with the increase in L than the first cumulant (see Figs. 2 and 3). Therefore, to simplify the discussion, we may consider that κ_2 and κ_3 are constants. As L increases, κ_1 increases, and, hence, the difference $I_{\rm th} - \kappa_1$ decreases. Consequently, the value of the Q-function increases, which means that the interference probability increases. However, κ_1 will converge to a constant with further increase in L, which implies that the interference probability will converge to a constant value as well.

C. Field Size and Spectrum-Sharing Opportunities

The discussion of the effect of the field size on spectrum-sharing opportunities is based on Fig. 7, which has a straight line that corresponds to a certain value of β. This line divides the figure into two main regions, i.e., interfering and noninterfering regions. If the maximum interference probability that a PU can tolerate is β (e.g., 0.1), then the aggregate interference generated by the secondary network is not considered to be harmful if the interference probability is less than β. Therefore, the part of Fig. 7 below the curve of $\beta = 0.1$ is considered to be a noninterfering region. In this case, a secondary network could concurrently and continuously share the spectrum with the PU. If the secondary network operates in the upper part of Fig. 7, i.e., the interfering region, the secondary network could utilize the spectrum during the absence of the PU. If the PU is present and active, then it is possible for the secondary network to access the spectrum, provided that it has adapted its operation parameters and has moved to the noninterfering region.

There are three curves in Fig. 7; each curve corresponds to a certain value of $I_{\rm th}$. For the curve corresponding to $I_{\rm th} = 0.009$,[3] the secondary network does not cause harmful interference toward the PU, regardless of the field size L. Therefore, expanding the field does not eliminate any spectrum-sharing opportunity. For the curve corresponding to $I_{\rm th} = 0.007$, on the other hand, the increase in L may move the secondary network from the noninterfering region to the interfering region, eliminating a spectrum-sharing opportunity. From the same curve and starting with a field with a large L, we may also deduce that a reduction in L might lead to moving the secondary network from the interfering region to the noninterfering region, which creates a spectrum-sharing opportunity. For the curve corresponding to $I_{\rm th} = 0.004$, a reduction in L never moves the secondary network from the interfering region to the noninterfering region, except when there is no transmitting node. Therefore, controlling the field size here does not create a spectrum-sharing opportunity.

Regarding the applicability of asymptotic results obtained for an infinite field to the case of a finite field, we can state the following: Asymptotic results obtained for infinite fields can be applied for finite fields whose radial depth L is much greater than the minimum distance between the field and the PU r_o. Otherwise, these asymptotic results will be too conservative and may lead to missing spectrum-sharing opportunities. In Fig. 7, where $r_o = 10$ m, the interference probability is almost constant, as long as $L > 1000$ m.

Due to space limitations, the effect of r_o on the interference probability and spectrum sharing is not discussed here (see [15]). However, it is worthwhile highlighting the following remarks. For lower r_o, the interference probability converges faster with respect to the increase in L. Furthermore, r_o is an important parameter in creating spectrum-sharing opportunities. A slight increase in r_o could move the operation of the secondary network to the noninterfering region and create a spectrum-sharing opportunity. This increase in r_o could be achieved by medium access control protocol, forcing nodes within a distance of r_o from the PU not to transmit.

VIII. Some Generalizations

The formulations and discussions presented in this paper can be generalized for the following cases:

Field with an irregular shape: If the PU-RX is inside a field of SU-TXs but the shape of this field is not a regular disk or annular sector shape, then the results obtained before are applicable to this case provided that the distance between the PU-RX and the nearest edge of the field is much greater than the radius of the exclusion region around the PU-RX. Otherwise, the field can be segmented into disjoint segments, and the total mth cumulant will be the sum of the mth cumulants of each segment, i.e., $\kappa_m = \sum_i \kappa_{m_i}$, where κ_{m_i} is the mth cumulant of segment i.

Heterogeneous networks: The results obtained before can be applied for a heterogeneous network (which can be visualized as the overlap of different types of networks). To illustrate this, let us assume that there are two overlapping, independent, and infinite networks, e.g., Net_1 and Net_2. Let us assume that each active node in Net_1 transmits P_1 W and that each active node in Net_2 transmits P_2 W. Let us assume that λ_1 and λ_2 denote the intensity of the active nodes in Net_1 and Net_2, respectively. Ignoring the effect of fading and other factors, the mth cumulant of the interference power due to the transmissions in Net_1 can be expressed as $\kappa_m(I_A, \text{Net}_1) = (2\pi/(nm-2))(\lambda_1 P_1^m / r_{o1}^{mn-2})$, where r_{o1} is the radius of the exclusion region for Net_1. Similarly, $\kappa_m(I_A, \text{Net}_2)$ can be written as $\kappa_m(I_A, \text{Net}_2) = (2\pi/(nm-2))(\lambda_2 P_2^m / r_{o2}^{mn-2})$. Therefore, the mth cumulant of the aggregate interference received by PU-RX at the origin becomes

$$\kappa_m(I_A) = \kappa_m(I_A, \text{Net}_1) + \kappa_m(I_A, \text{Net}_2)$$
$$= \frac{2\pi}{nm-2}\left(\frac{\lambda_1 P_1^m}{r_{o1}^{mn-2}} + \frac{\lambda_2 P_2^m}{r_{o2}^{mn-2}}\right). \quad (16)$$

[3]All values of $I_{\rm th}$ mentioned here and in Fig. 7 are normalized with respect to the deterministic parts of I_A, e.g., transmit power and antenna gains, which are not of our interest in this discussion. The values of $I_{\rm th}$ are properly chosen from the corresponding CCDF curve (see, e.g., Fig. 4).

Many PUs: While the system model considers a single PU-RX, results of this paper are still useful for cases having many PU-RXs (composing a primary network). For example, if a primary network allows spectrum sharing only if none of its PU-RXs is experiencing harmful interference, then analysis in this paper should be applied to the PU-RX representing the worst-case scenario. An example of a PU-RX representing the worst-case scenario is when the primary network and secondary network partially overlap at the edges. In this case, the deepest PU-RX within the secondary network will be considered for the analysis.

IX. Conclusion

In this paper, we have characterized the aggregate interference power generated by a secondary network through a cumulant-based approach. We have introduced a simple yet comprehensive method for calculating the cumulants. Our method is applicable for finite and infinite secondary networks and is flexible to encompass different system and propagation parameters, including large-scale fading, small-scale fading, and composite fading. We have also discussed the behavior of these cumulants with respect to changes in the network size and fading distributions. Moreover, we have highlighted some cumulant-based approximations of the distribution of the aggregate interference power. One main contribution of this paper is the study of the impact of the field size of secondary users on spectrum-sharing opportunities. The study shows that an increase in the field size may eliminate the spectrum-sharing opportunities. However, there are some cases where the spectrum-sharing opportunities are not reduced by the increase in the field size, even when the field size grows to infinity. This paper has demonstrated that asymptotic results obtained for an infinite field could be applied for a finite field whose radial depth is much greater than the minimum distance between the field and the PU. Otherwise, these asymptotic results will be too conservative and may lead to missed spectrum-sharing opportunities.

Appendix A

Multipath fading: A general model that could be used to reflect multipath fading on the interference power is the Gamma distribution (under the assumption of Nakagami fading for the interference signal). The pdf of Gamma distribution is $f_X(x) = (\nu/\Omega)^\nu (x^{\nu-1}/\Gamma(\nu)) e^{-(\nu/\Omega)x}$, $x > 0$, $\nu \geq (1/2)$, where ν is the shape parameter, $\Gamma(.)$ is the Gamma function, and Ω is the average power, i.e., $E[X]$, which is commonly assumed to be equal to unity [18]. The characteristic function of this Gamma random variable can be written as [19] $\phi_X(\omega) = (1/(1 - j\omega(\Omega/\nu))^\nu)$. Therefore, $\tilde{\mu}_m(X) = (\ 1/j^m\ )[(\ d^m \phi_X(\omega)/d\omega^m\ )]_{\omega\,=\,0} = (\Omega/\nu)^m \prod_{l=0}^{m-1}(\nu + l)$. Using $\prod_{l=0}^{m-1}(\nu + l) = \Gamma(\nu + m)/\Gamma(\nu)$, for m, which is a positive integer [20], we can rewrite $\tilde{\mu}_m(X)$ as $\tilde{\mu}_m(X) = (\Omega/\nu)^m(\Gamma(\nu + m)/\Gamma(\nu))$. From this expression of $\tilde{\mu}_m(X)$, (4), and (8), and considering $\Omega = 1$, the cumulants of I_A can be expressed as

$$\kappa_m(I_A) = N_{\text{eff}}(m)\,[g(r_o)]^m\,\nu^{-m}\frac{\Gamma(\nu+m)}{\Gamma(\nu)}. \tag{17}$$

Shadow fading: The shadow fading is usually modeled by a log-normal random variable $X_i = 10^{S_i/10}$, where S_i is a normal random variable with zero mean and a standard deviation of σ_{dB}. Since we assume that X_i's are identically distributed, we omit subscript i in the following derivation. It is more convenient to write X as $X = e^Z$, where Z is a normal random variable whose mean and standard deviation are μ_Z and σ_Z, respectively. We will start by deriving the raw moments of X in terms of the moments of Z. From [19], the pdf of the random variable X can be written as $f_X(x) = (1/\sigma_Z\ x\sqrt{2\pi}) e^{-((\ln(x)-\mu_Z)^2/2\sigma_Z^2)}$, $x > 0$. Therefore

$$\tilde{\mu}_m(X) = \mathbb{E}[X^m] = \int_0^\infty x^m \frac{1}{\sigma_Z\ x\sqrt{2\pi}} e^{-\frac{(\ln(x)-\mu_Z)^2}{2\sigma_Z^2}}\,dx. \tag{18}$$

By making $y = \ln(x) - \mu_Z$, (18) can be rewritten in terms of y as

$$\tilde{\mu}_m(X) = \int_{-\infty}^\infty \frac{1}{\sigma_Z\ \sqrt{2\pi}} e^{-\left(\frac{y^2}{2\sigma_Z^2} - my - m\,\mu_Z\right)}\,dy. \tag{19}$$

Since $\int_{-\infty}^{\infty} e^{-(ay^2+by+c)}dy = \sqrt{\pi/a}e^{(b^2-4ac)/4a}$, (19) yields $\tilde{\mu}_m(X) = e^{m\mu_Z + (1/2)m^2\sigma_Z^2}$. From $X = 10^{S/10} = e^Z$, we have $\mu_Z = \mu_S(\ln 10/10) = 0$ and $\sigma_Z^2 = \sigma_{\text{dB}}^2(\ln 10/10)^2$. Therefore, $\tilde{\mu}_m(X) = e^{(1/2)(m(\ln 10/10)\sigma_{\text{dB}})^2}$. Using (4), (8), and this expression of $\tilde{\mu}_m(X)$, we can write $\kappa_m(I_A)$ as (after some normalization)

$$\kappa_m(I_A) = N_{\text{eff}}(m)\,[g(r_o)]^m\,e^{\frac{1}{2}\left(m\frac{\ln 10}{10}\sigma_{\text{dB}}\right)^2}. \tag{20}$$

Appendix B

The skewness ρ of I_A can be expressed as $\rho = \kappa_3(I_A)/[\kappa_2(I_A)]^{3/2}$. Recalling that $\kappa_m(I_A) = N_{\text{eff}}(m)g(r_o)^m\tilde{\mu}_m(X)$, the skewness of I_A becomes $\rho = N_{\text{eff}}(3)\tilde{\mu}_3(X)/[N_{\text{eff}}(2)\tilde{\mu}_2(X)]^{3/2}$. The effect of the spatial distribution of the secondary network on the skewness of I_A is reflected by the ratio $N_{\text{eff}}(3)/[N_{\text{eff}}(2)]^{3/2}$. Let $\acute{\rho}$ denote this ratio, i.e., $\acute{\rho} = N_{\text{eff}}(3)/[N_{\text{eff}}(2)]^{3/2}$. Substituting the expressions of $N_{\text{eff}}(2)$ and $N_{\text{eff}}(3)$ into this expression of $\acute{\rho}$ yields (after some simplification) (21), shown at the bottom of the page. From (21), it is clear that the skewness decreases with the increase in λ or θ. However, the maximum value of θ is 2π; therefore, its effect is limited. What matters in the effect of L on the skewness is the ratio of L to r_o

$$\acute{\rho} = \begin{cases} \frac{1}{\sqrt{\lambda\theta r_o^2}}\,\frac{(2n-2)^{3/2}}{3n-2}\,\frac{1-\left(\frac{r_o}{r_o+L}\right)^{3n-2}}{\left[1-\left(\frac{r_o}{r_o+L}\right)^{2n-2}\right]^{3/2}}, & \text{for } 0 < r_c \leq r_o \leq r_o + L \\ \frac{1}{\sqrt{\lambda\theta r_c^2}}\,\frac{\frac{1}{2}\left(1-\frac{r_o^2}{r_c^2}\right)+\frac{1}{3n-2}\left[1-\left(\frac{r_c}{r_o+L}\right)^{3n-2}\right]}{\left(\frac{1}{2}\left(1-\frac{r_o^2}{r_c^2}\right)+\frac{1}{2n-2}\left[1-\left(\frac{r_c}{r_o+L}\right)^{2n-2}\right]\right)^{3/2}}, & \text{for } 0 \leq r_o < r_c \leq r_o + L \\ \frac{1}{\sqrt{\frac{1}{2}\lambda\theta\left[(r_o+L)^2 - r_o^2\right]}}, & \text{for } 0 \leq r_o \leq r_o + L < r_c \end{cases} \tag{21}$$

or r_c. A more detailed discussion about the skewness of I_A is included in [12], mainly in Section III.

ACKNOWLEDGMENT

The authors would like to thank Dr. S. Al-Ahmadi and Dr. S. Szyszkowicz from Carleton University for their helpful comments.

REFERENCES

[1] M. Aljuaid and H. Yanikomeroglu, "Impact of secondary users' field size on spectrum sharing opportunities," in *Proc. IEEE WCNC*, Sydney, Australia, Apr. 2010, pp. 1–6.
[2] M. Aljuaid and H. Yanikomeroglu, "A cumulant-based characterization of the aggregate interference power in wireless networks," in *Proc. IEEE VTC—Spring*, Taipei, Taiwan, May 2010, pp. 1–5.
[3] Fed. Commun. Comm., *Spectrum Policy Task Force*, Nov. 2002, ET Docket no. 02-135.
[4] R. Menon, R. M. Buehrer, and J. H. Reed, "Outage probability based comparison of underlay and overlay spectrum sharing techniques," in *Proc. 1st IEEE Symp. DySPAN*, Baltimore, MD, Nov. 2005, pp. 101–109.
[5] P. C. Pinto and M. Z. Win, "Spectral characterization of wireless networks," *IEEE Wireless Commun.*, vol. 14, no. 6, pp. 27–31, Dec. 2007.
[6] A. Ghasemi and E. S. Sousa, "Interference aggregation in spectrum-sensing cognitive wireless networks," *IEEE J. Sel. Topics Signal Process.*, vol. 2, no. 1, pp. 41–56, Feb. 2008.
[7] M. Z. Win, P. C. Pinto, and L. A. Shepp, "A mathematical theory of network interference and its applications," *Proc. IEEE*, vol. 97, no. 2, pp. 205–230, Feb. 2009.
[8] M. Haenggi, J. G. Andrews, F. Baccelli, O. Dousse, and M. France schetti, "Stochastic geometry and random graphs for the analysis and design of wireless networks," *IEEE J. Sel. Areas Commun.*, vol. 27, no. 7, pp. 1029–1046, Sep. 2009.
[9] E. Salbaroli and A. Zanella, "Interference analysis in a Poisson field of nodes of finite area," *IEEE Trans. Veh. Technol.*, vol. 58, no. 4, pp. 1776–1783, May 2009.
[10] C. C. Chan and S. V. Hanly, "Calculating the outage probability in a CDMA network with spatial Poisson traffic," *IEEE Trans. Veh. Technol.*, vol. 50, no. 1, pp. 183–204, Jan. 2001.
[11] R. Menon, R. M. Buehrer, and J. H. Reed, "Impact of exclusion region and spreading in spectrum-sharing ad hoc networks," in *Proc. 1st Int. Workshop Technol. Policy Access. Spectrum*, Boston, MA, Aug. 2006.
[12] M. Aljuaid and H. Yanikomeroglu, "Investigating the Gaussian convergence of the distribution of the aggregate interference power in large wireless networks," *IEEE Trans. Veh. Technol.*, vol. 59, no. 9, pp. 4418–4424, Nov. 2010.
[13] H. Inaltekin, M. Chiang, H. V. Poor, and S. B. Wicker, "On unbounded path-loss models: Effects of singularity on wireless network performance," *IEEE J. Sel. Areas Commun.*, vol. 27, no. 7, pp. 1078–1091, Sep. 2009.
[14] A. Hasan and J. G. Andrews, "The guard zone in wireless ad hoc networks," *IEEE Trans. Wireless Commun.*, vol. 6, no. 3, pp. 897–906, Mar. 2007.
[15] M. Aljuaid, "Interference characterization and spectrum sharing in large wireless networks," Ph.D. dissertation, Carleton Univ., Ottawa, ON, Canada, Jul. 2010.
[16] R. K. Ganti and M. Haenggi, "Interference in ad hoc networks with general motion-invariant node distribution," in *Proc. IEEE ISIT*, Toronto, Canada, Jul. 2008, pp. 1–5.
[17] D. E. Barton and K. E. Dennis, "The conditions under which Gram-Charlier and Edgeworth curves are positive definite and unimodal," *Biometrika*, vol. 39, no. 3/4, pp. 425–427, 1952.
[18] P. M. Shankar, "Performance analysis of diversity combining algorithms in shadowed-fading channels," *Wireless Pers. Commun.*, vol. 37, no. 1/2, pp. 61–72, Apr. 2006.
[19] A. Papoulis, *Probability, Random Variables and Stochastic Processes*. New York: McGraw-Hill, 1991.
[20] E. W. Weisstein, *Gamma Function From MathWorld–A Wolfram Web Resource*. [Online]. Available: http://functions.wolfram.com/06.05.16.0020.01

Novel Partial Selection Schemes for AF Relaying in Nakagami-m Fading Channels

Yunfei Chen, *Senior Member, IEEE*, Cheng-Xiang Wang, *Senior Member, IEEE*, Hailin Xiao, and Dongfeng Yuan, *Senior Member, IEEE*

***Abstract*—New partial relay selection schemes for cooperative diversity based on amplify-and-forward (AF) relaying are proposed in Nakagami-m fading channels. Their performances are compared with the conventional partial selection scheme. Numerical results show that the new schemes have performance gains of up to 5 dB over the conventional scheme. In some cases, their performances are indistinguishable from the full selection scheme, but they have much simpler structures. Numerical results also show that it is more important to choose the idle user for the hop with a small average signal-to-noise ratio (SNR) or an m parameter in partial selection. Based on this observation, a new adaptive partial selection scheme based on the average SNR, and the m parameter is derived. A complexity analysis also shows that the new schemes reduce the complexity in some cases.**

***Index Terms*—Amplify-and-forward (AF), performance analysis, user selection.**

I. INTRODUCTION

In recent years, cooperative diversity has been proposed as an effective method of improving the performance of a wireless system [1]. In a cooperative diversity system, idle users are employed to forward signals from the source to the destination. The idle users act as virtual antennas to achieve cooperative space diversity at the destination, in contrast to the traditional diversity system where multiple antennas are physically installed at the destination [2]–[5]. Among all the existing protocols for cooperative diversity, amplify-and-forward (AF) relaying is one of the simplest protocols [1]. The performance of AF cooperative diversity improves as the number of idle users increases [6]. However, the complexity of the network also increases as the number of the idle users increases. In some applications,

Manuscript received February 10, 2011; revised April 12, 2011 and May 24, 2011; accepted June 4, 2011. Date of publication June 16, 2011; date of current version September 19, 2011. The work of Y. Chen was supported by the Engineering and Physical Sciences Research Council First Grant. The work of C.-X. Wang and D. Yuan was supported by the Research Councils UK (RCUK) for the U.K.–China Science Bridges: R&D on (B)4G Wireless Mobile Communications. The work of H.-L. Xiao was supported in part by the National Basic Research Program of China "973" under Grant 2008CB317109, by Guangxi Natural Science Foundation under Grant 2011GXNSFD018028, by the Guangxi Science Foundation under Grant 0991241, by the National Natural Science Foundation of China under Grant 60872022 and Grant 60972084, and by the Foundation of Guangxi Key Laboratory of Information and Communication under Grant 10903. The work of C.-X. Wang and H.-L. Xiao was supported in part by the Guangxi Natural Science Foundation under Grant 2011GXNSFD018028 and in part by the Opening Project of the Key Laboratory of Cognitive Radio and Information Processing (Guilin University of Electronic Technology), Ministry of Education, under Grant 2009K02. The review of this paper was coordinated by Prof. W. A. Hamouda.

Y. Chen is with the School of Engineering, University of Warwick, Coventry CV4 7AL, U.K. (e-mail: Yunfei.Chen@warwick.ac.uk).
C.-X. Wang is with the Joint Research Institute for Signal and Image Processing, School of Engineering and Physical Sciences, Heriot-Watt University, Edinburgh EH14 4AS, U.K. (e-mail: Cheng-Xiang.Wang@hw.ac.uk).
H. Xiao is with the School of Information and Communication, Guilin University of Electronic Technology, Guilin 541004, China (e-mail: xhl_xiaohailin@yahoo.com.cn).
D. Yuan is with the School of Information Science and Engineering, Shandong University, Jinan 250100, China (e-mail: dfyuan@sdu.edu.cn).

Digital Object Identifier 10.1109/TVT.2011.2159637